

Arteriosclerosis, Thrombosis, and Vascular Biology



JOURNAL OF THE AMERICAN HEART ASSOCIATION

Trophoblast-Induced Changes in C-X-C Motif Chemokine 10 Expression Contribute to Vascular Smooth Muscle Cell Dedifferentiation During Spiral Artery Remodeling
Alison E. Wallace, Judith E. Cartwright, Runa Begum, Ken Laing, Baskaran Thilaganathan and Guy S. Whitley

Arterioscler Thromb Vasc Biol. 2013;33:e93-e101; originally published online January 3, 2013;
doi: 10.1161/ATVBAHA.112.300354

Arteriosclerosis, Thrombosis, and Vascular Biology is published by the American Heart Association, 7272
Greenville Avenue, Dallas, TX 75231

Copyright © 2013 American Heart Association, Inc. All rights reserved.
Print ISSN: 1079-5642. Online ISSN: 1524-4636

The online version of this article, along with updated information and services, is located on the
World Wide Web at:

<http://atvb.ahajournals.org/content/33/3/e93>

Data Supplement (unedited) at:

<http://atvb.ahajournals.org/content/suppl/2013/01/03/ATVBAHA.112.300354.DC1.html>

Permissions: Requests for permissions to reproduce figures, tables, or portions of articles originally published in *Arteriosclerosis, Thrombosis, and Vascular Biology* can be obtained via RightsLink, a service of the Copyright Clearance Center, not the Editorial Office. Once the online version of the published article for which permission is being requested is located, click Request Permissions in the middle column of the Web page under Services. Further information about this process is available in the [Permissions and Rights Question and Answer](#) document.

Reprints: Information about reprints can be found online at:
<http://www.lww.com/reprints>

Subscriptions: Information about subscribing to *Arteriosclerosis, Thrombosis, and Vascular Biology* is online at:
<http://atvb.ahajournals.org/subscriptions/>

Trophoblast-Induced Changes in C-X-C Motif Chemokine 10 Expression Contribute to Vascular Smooth Muscle Cell Dedifferentiation During Spiral Artery Remodeling

Alison E. Wallace, Judith E. Cartwright, Runa Begum, Ken Laing, Baskaran Thilaganathan, Guy S. Whitley

Objective—During pregnancy, fetal trophoblast disrupt endothelial cell and vascular smooth muscle cell (VSMC) interactions in spiral arteries of the maternal decidua to enable increased nutritional and oxygen delivery to the fetus. Little is known regarding this transformation because of difficulties of studying human pregnancy in vivo. This study investigated how trophoblast-secreted factors affect the interactions of vascular cells and the differentiation status of VSMC during spiral arteries remodeling using 3-dimensional vascular spheroid coculture.

Methods and Results—Endothelial cell and VSMC were cocultured in hanging droplets to form spheroids representing an inverted vessel lumen. Control or conditioned media from an extravillous trophoblast (EVT) cell line was incubated with vascular spheroids for 24 hours. Spheroid RNA was then analyzed by Illumina Sentrix BeadChip array. Spheroids incubated with EVT conditioned medium showed significant up/downregulation of 101 genes (>1.5-fold; $P < 0.05$), including an upregulation of C-X-C motif chemokine 10 (IP-10). C-X-C motif chemokine 10 expression was confirmed by qualitative real-time PCR and Western blot analysis of spheroids, and immunohistochemistry of first trimester decidua and ex vivo dissected nonplacental bed spiral arteries. EVT conditioned medium reduced VSMC expression of differentiation markers, and both EVT conditioned medium and C-X-C motif chemokine 10 increased motility of VSMC indicating dedifferentiation of VSMC.

Conclusion—EVT-induced C-X-C motif chemokine 10 expression may contribute to spiral arteries remodeling during pregnancy by altering the motility and differentiation status of the VSMC in the vessel. (*Arterioscler Thromb Vasc Biol.* 2013;33:e93-e101)

Key Words: CXCL10/IP-10 ■ spiral artery remodeling ■ 3D culture ■ trophoblast ■ vascular smooth muscle cell

During the first trimester of pregnancy, spiral arteries (SA) within the maternal uterus (decidua and myometrium) are remodeled from small diameter vessels with a low flow at high resistance, to those with a large diameter and high flow at low resistance. This transformation results in vessels that are not responsive to vasoconstrictors and provide increased blood flow to the fetus at a reduced pressure. Complete physiological remodeling of the SA is achieved only in the presence of fetal extravillous trophoblast (EVT).¹ EVT are specialized cells that migrate both into the decidual stroma and retrograde to flow in the lumen of SA, where they are termed endovascular trophoblast.² Endovascular trophoblast disrupt the interactions of the endothelial cells (EC) and vascular smooth muscle cells (VSMC) making up the SA, and eventually mediate the loss of these cells through mechanisms thought to involve apoptosis and dedifferentiation.³ Endovascular trophoblast then replace the cells they have displaced, and adopt a more endothelial-like phenotype,⁴ before reendothelialization occurs.

Defects in this unique remodeling process have been associated with the onset of pregnancy disorders, including

preeclampsia, intrauterine growth restriction, and preterm labor. Although the symptoms of these disorders commonly present later in pregnancy, inadequate SA remodeling is proposed to occur during the first trimester.⁵ Relatively little is known regarding the mechanisms of normal SA remodeling because of the difficulties of studying early human pregnancy. Animal models are limited because of the lack of deep trophoblast invasion and SA transformation in other species.⁶ Therefore, there is a need to model these multicellular interactions in vitro. Previous models include the use of monolayer cocultures,⁷ explant cultures,⁸ and endothelial capillary tubes on Matrigel.⁹ These have revealed the secretion of a number of factors by endovascular trophoblast which impact on the physiological changes that occur in SA remodeling, including the secretion of proteases to degrade the extracellular matrix and disrupt cellular interactions,¹⁰ and chemokines including interleukin (IL)-8, MCP-1,¹¹ and IL-6.¹² Trophoblast also induce reduced expression and disruption of EC adhesion molecules, such as E-cadherin,¹³ and apoptosis of vascular cells.^{14,15}

Received on: August 24, 2012; final version accepted on: December 13, 2012.

From the Division of Biomedical Sciences, Reproductive and Cardiovascular Disease Research Group, St George's University of London, United Kingdom (A.E.W., J.E.C., R.B., B.T., G.S.W.); Division of Clinical Sciences, Infection & Immunity Research Centre, St Georges University of London, United Kingdom (K.L.); and Fetal Medicine Unit, St George's Hospital, United Kingdom (B.T.).

The online-only Data Supplement is available with this article at <http://atvb.ahajournals.org/lookup/suppl/doi:10.1161/ATVBAHA.112.300354/-/DC1>.

Correspondence to Professor Guy Whitley, Division of Biomedical Sciences, Reproductive and Cardiovascular Disease Research Group, St George's University of London, Cranmer Terrace, SW17 0RE, United Kingdom. E-mail gwhitley@sgul.ac.uk

© 2013 American Heart Association, Inc.

Arterioscler Thromb Vasc Biol is available at <http://atvb.ahajournals.org>

DOI: 10.1161/ATVBAHA.112.300354

Furthermore, EC and VSMC are not passive observers of the remodeling process and respond to trophoblast with alterations in protease production,¹⁶ cell motility,¹⁷ adhesion properties,¹² and cytokine production.¹¹

The use of 3-dimensional (3D) spheroid cell culture models may overcome some limitations of both monolayer cells and ex vivo explants in studying the initial stages of human placentation, as cells grown in 3D cultures retain a phenotype more similar to in vivo than in monolayer.¹⁸ Vascular spheroids show some of the phenotypic properties of vessels, such as differentiation of EC as demonstrated by a downregulation of platelet-derived growth factor expression, CD34 expression, and a reduction in apoptosis.¹⁹ A similarity to the structure of the vessel wall is also retained, with a monolayer of EC over a core of VSMC, however limitations are presented by the lack of connective tissue and shear stress present in a vessel. In this study, we used this 3D multicellular model to investigate changes in gene expression within the vasculature in response to trophoblast secreted factors using a genome-wide microarray. Expression of C-X-C motif chemokine 10 (CXCL10; previously known as IP-10), a protein found to be upregulated in the array, has been reported in both EC and VSMC in response to proinflammatory stimuli,^{20,21} as well as some uterine EC in vivo.²² CXCL10 has also previously been implicated in vessel destabilization, and therefore we investigated its role in SA remodeling and found that IFN- γ may be involved in the induction of CXCL10 in SA, and that EVT conditioned medium (CM) and CXCL10 contribute toward VSMC dedifferentiation and motility, key steps in the remodeling process.

Materials and Methods

Expanded methods are available in the online-only Data Supplement.

Cell Culture

The human vascular smooth muscle cell line SGHVSMC-9 (VSMC), human endothelial cell line SGHEC-7 (EC), and human EVT cell line SGHPL-4 were maintained, as previously described.^{15,23,24}

Generation of EVT CM

SGHPL-4 cells were grown in 3D culture, as previously described,²⁴ and CM collected after 24 hours, as described in the Methods in the online-only Data Supplement.

Spheroid Generation

To generate spheroids, a hanging drop VSMC/EC coculture (750 cells each) method was used.^{25,26}

Microarray Analysis

RNA isolation, microarray analysis, and SYBR green quantitative real-time PCR was carried out, as described in the Methods in the online-only Data Supplement.

Western Blot Analysis

Spheroids (n=64) and monolayer VSMC were lysed in 50 μ L RIPA buffer and Western blot analysis was carried out by standard procedure using rabbit anti-CXCL10, mouse anti α -smooth muscle actin, or rabbit anticalponin.

Ex Vivo Vessel Explant Model

Informed consent was obtained and ethical committee approval was in place for all studies. Decidual/myometrial biopsies (n=3) were obtained from nonplacental bed areas from pregnant women undergoing elective Caesarean section at term for reasons such as breech presentation. SA were dissected, as previously described.⁸ Vessels were incubated with EVT CM for 24 hours, when arteries were cryo-sectioned for immunohistochemical staining.

Immunohistochemistry

All immunohistochemistry was carried out by standard procedures described in the online-only Data Supplement.

Microscopy

Confocal and time-lapse microscopy was carried out, as described in the online-only Data Supplement.

Statistical Analysis

Nonparametric statistical analysis was applied where appropriate. Mann-Whitney tests were used to analyze quantitative PCR data, and the Friedman test with Dunns post hoc test was used to analyze experiments with multiple variables. Analysis was carried out using GraphPad Prism (GraphPad Software, San Diego, CA). Data are presented as mean \pm SEM.

Results

Vascular Spheroids Form a Monolayer of EC Surrounding a Core of VSMC

To investigate the effect of trophoblast on the interaction of EC and VSMC in the remodeling SA, we used coculture vascular spheroids. To confirm that the orientation of EC and VSMC modeled a vessel, EC and VSMC were fluorescently labeled for confocal imaging. After 24 hours, the EC orientated to the exterior of the spheroid in a monolayer, as previously described (Figure 1A),¹⁹ whereas the VSMC formed an internal core (Figure 1B). This culture system reestablished the orientation and cellular interactions between the EC monolayer and the underlying VSMC seen in the intact vessel in vivo (Figure 1C), and therefore was used to model the effects of endovascular trophoblast within the lumen of SA.

101 Genes Were Significantly Altered by Trophoblast CM

To analyze changes in gene expression in the vasculature induced by trophoblast-secreted factors, trophoblast CM generated from the EVT cell line SGHPL-4 grown in 3D was added to vascular spheroids and incubated for 24 hours. The resulting cRNA was hybridized to Illumina Sentrix BeadChip Array and data analyzed, as described in the Methods in the online-only Data Supplement. The comparison revealed 101 genes that were significantly altered >1.5-fold in CM-treated vascular spheroids as compared with control (C)-treated vascular spheroids ($P<0.05$; Table I in the online-only Data Supplement). Of these, 9 were downregulated and 92 were upregulated. A total of 10 genes showed a significant upregulation of over >2-fold ($P<0.05$; Table). These genes were members of diverse families, which included cytokines, chemokines, and growth factors and included of particular interest chemokine (C-X-C motif) ligand 10 (CXCL10), chemokine

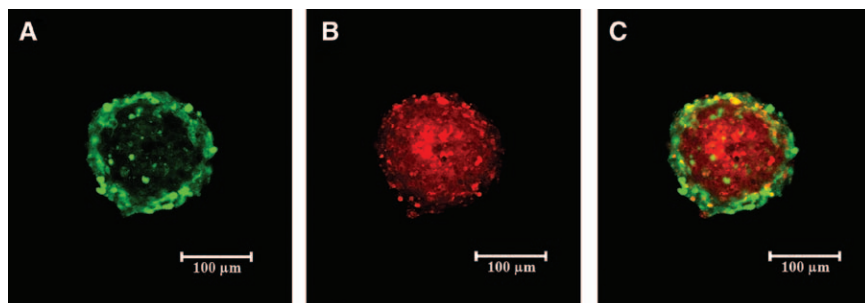


Figure 1. Endothelial cell (EC) and vascular smooth muscle cell (VSMC) spontaneously orientate to mimic features of a vessel lumen. (A) EC (green channel) and (B) VSMC (red channel) were cocultured in equal numbers in hanging droplets to form 3-dimensional (3D) vascular spheroid cocultures (C, merge) and examined by confocal microscopy.

(C-C motif) ligand 20, stanniocalcin-1, IL-6, CD93, IL-11, platelet-derived growth factor, and placental growth factor. The full list was further analyzed by gene ontology analysis, and this revealed 36 significant biological processes ($P < 0.05$) each containing between 2 and 54 genes (listed in full in Table II in the online-only Data Supplement). Of interest were ontologies relating to both cell proliferation and negative proliferation, response to wounding, various ontologies relating to signaling (including signal transduction, cell communication, cell-cell signaling), inflammatory response, and cell migration as well as some vascular processes (including angiogenesis, blood vessel development, and vascular development).

Microarray Verification

To verify the results of the array, quantitative real-time PCR was performed for the transcripts of CXCL10 (Figure 2A), stanniocalcin-1 (Figure 2B), and placental growth factor (Figure 2C) using independently isolated RNA samples to those used for array analysis. This analysis confirmed a statistically significant increase in mRNA expression in CM-treated vascular spheroids of CXCL10 (7.9-fold, $P < 0.05$; Figure 2A), stanniocalcin-1 (2.3-fold, $P < 0.05$; Figure 2B), and placental growth factor (3.4-fold, $P < 0.05$; Figure 2C), as compared with control-treated spheroids. A time course over 48 hours was carried out to examine CXCL10 mRNA expression, which was found to peak at 24 hours (Figure I in the online-only Data Supplement).

CXCL10 Protein Is Expressed by Vascular Spheroids in Response to Trophoblast CM

The expression of CXCL10 was chosen for further investigation, as it has previously been implicated in vessel

destabilization in other vascular beds, however, mostly relating to its effects on EC.^{27,28} To further confirm the upregulation of CXCL10 by EVT CM in vascular spheroids, Western blot analysis was performed. Spheroids were formed of EC alone, VSMC alone, and in coculture. After 24 hours treatment, there was a small increase in CXCL10 protein expression when EC or VSMC were cultured alone, although this did not reach statistical significance. When EC and VSMC were cocultured in spheroids, there was a significant increase in CXCL10 expression of 3.7-fold in EC/VSMC spheroids treated with CM as compared with control ($P < 0.05$; Figure 3A). The fold increase in CXCL10 protein expression in EC/VSMC spheroids was greater than the additive effect of the cell types cultured separately.

CXCL10 protein expression was also investigated by immunocytochemistry in vascular spheroids treated with control media or EVT CM. Cells positive for CXCL10 expression could be identified in sections of spheroids treated with control media (Figure 3B), however increased CXCL10 immunoreactivity was observed in vascular spheroids treated with EVT CM (Figure 3C). This appeared primarily to be present in the VSMC core; however, it could also be identified in the EC.

CXCL10 Expression in Ex Vivo SA and First Trimester Decidua

To confirm the expression of CXCL10 in a physiological setting, CXCL10 protein was examined by immunohistochemistry of serial sections of first trimester decidua. CXCL10 immunoreactivity was found widely throughout the stroma in all decidua sections examined ($n = 5$; Figure 4A, and magnification Figure 4C). We could colocalize CXCL10 expression with α -smooth muscle actin expression, indicating CXCL10

Table. Vascular Spheroid Gene Expression Altered >2-Fold by Trophoblast Conditioned Media

Gene Name/Symbol	Fold Change (Absolute)	Up/Down	Corrected <i>P</i> Value
Homo sapiens CD93 molecule (CD93)	2.59	up	0.00625
Homo sapiens stanniocalcin 1 (STC1)	2.34	up	0.00188
Homo sapiens chemokine (C-C motif) ligand 20 (CCL20)	2.27	up	0.03741
Homo sapiens podocalyxin-like (PODXL), transcript variant 1	2.27	up	0.01122
Homo sapiens chemokine (C-X-C motif) ligand 10 (CXCL10)	2.24	up	0.02034
Homo sapiens interleukin 6 (interferon, beta 2) (IL6)	2.202	up	0.0266
Homo sapiens tissue factor pathway inhibitor 2 (TFPI2)	2.20	up	0.01540
Homo sapiens transmembrane protein 158 (TMEM158)	2.15	up	0.00625
Homo sapiens interleukin 11 (IL11)	2.14	up	0.00866
Homo sapiens placental growth factor (PGF)	2.01	up	0.01540

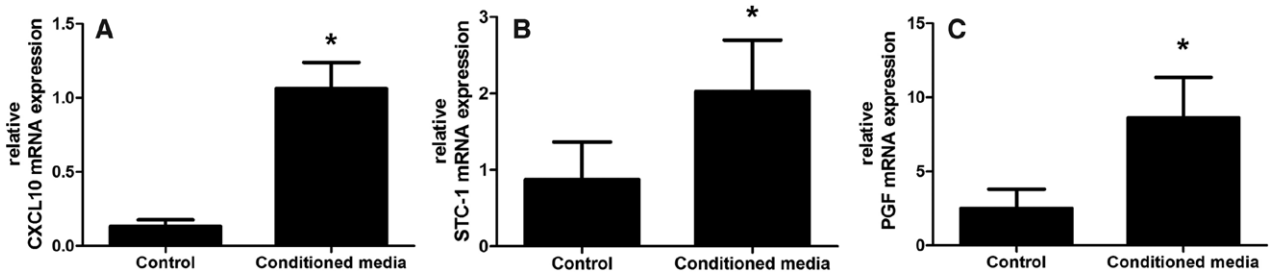


Figure 2. C-X-C motif chemokine 10 (CXCL10), stanniocalcin-1, and placental growth factor mRNA expression is significantly increased by trophoblast conditioned media (CM). Messenger RNA expression in vascular spheroids was measured by quantitative real-time PCR after stimulation with trophoblast CM for 24 hours (n=4). Data are expressed as mRNA expression relative to an external calibrator. **A**, CXCL10. **B**, Stanniocalcin-1. **C**, Placental growth factor. All data are presented as mean±SEM. *P<0.05.

expression by VSMC (Figure 4C and 4D, marked by arrowheads). Interestingly, cells expressing both smooth muscle actin and CXCL10 were also found a small distance away from the lumen of the artery. This was at a time when trophoblasts were present in the decidua (CK7 immunohistochemistry, B). CXCR3 expression was also examined in the decidua, and was also found to be localized to α-smooth muscle actin expression at a time when trophoblasts were present in the decidua (Figure II in the online-only Data Supplement).

The role of EVT CM in inducing expression of CXCL10 was then examined in SA isolated from biopsies of nonplacental bed decidua/myometrium. SA were dissected and incubated with EVT CM for 24 hours. CXCL10 protein expression was examined by immunohistochemistry (Figure 4). Expression of CXCL10 (green channel) in the EC (red channel, identified by VWF immunostaining) and VSMC component (merge) was identified in arteries treated with EVT CM (Figure 4E–4G).

CXCL10 Expression Is Partly Induced by IFN-γ

IFN-γ is a well-known stimulant of CXCL10, and recombinant IFN-γ can induce CXCL10 expression in vascular spheroids (Figure 5A). Previous studies have shown that EVT secrete IFN-γ.²⁹ We next examined whether IFN-γ in EVT CM was responsible for the induction of CXCL10 expression in the vascular spheroids. When IFN-γ was removed from EVT CM (using an IFN-γ-blocking antibody), before incubation with EC/VSMC spheroids for 24 hours, CXCL10 expression was reduced by an average of 4.5-fold as compared with CM incubated with control mouse IgG (P<0.05; Figure 5B).

Effect of CXCL10 and EVT CM on VSMC

CXCL10 has been previously shown to alter functional dedifferentiation markers of VSMC, including motility.³⁰ During SA remodeling, this process may play a key role. Therefore, to determine a potential effect on SA of CXCL10 production, recombinant CXCL10 or EVT CM was added to cultures of VSMC for a period of 24 or 72 hours. The differentiation markers α-smooth muscle actin and calponin, motility and proliferation of VSMC were assessed after 72 hours. EVT CM significantly decreased the expression of α-smooth muscle actin (Figure 6A) and calponin (Figure 6B), indicating a switch to a noncontractile, dedifferentiated phenotype. Recombinant CXCL10 induced a small decrease in expression of these markers that did not reach statistical significance. Motility of VSMC was significantly and dose-dependently

increased over 24 hours in response to CXCL10 (Figure 6C; 10 ng: 1.4-fold; 100 ng: 1.57-fold, P<0.05; 200 ng: 1.61-fold). Treatment of VSMC with EVT CM for 24 hours also significantly increased cell motility (Figure 6D; 71 ng protein/μL: 1.67-fold; 141 ng protein/μL: 1.9-fold, P<0.05).

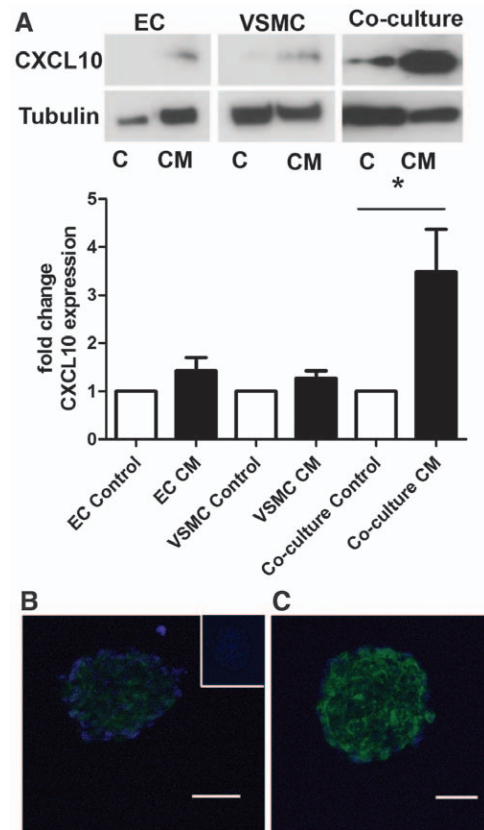


Figure 3. C-X-C motif chemokine 10 (CXCL10) protein is expressed by vascular spheroids stimulated with trophoblast conditioned media. **A**, Vascular spheroid lysates were examined by Western blot analysis for the presence of CXCL10. Tubulin was used as an internal loading control. The image shown is representative of 3 independent experiments. Densitometric analysis of Western blots (n=3) with mean±SEM CXCL10/tubulin presented as a fold-change over control-treated spheroids. *P<0.05. Vascular spheroids treated with control media (**B**) or trophoblast conditioned media (**C**) were cryosectioned and sections were examined by immunostaining for the presence of CXCL10. Sections were taken through approximately the center of the spheroid. Negative control incubated with rabbit IgG in place of primary antibody is inset. Scale bar, 100 μm.

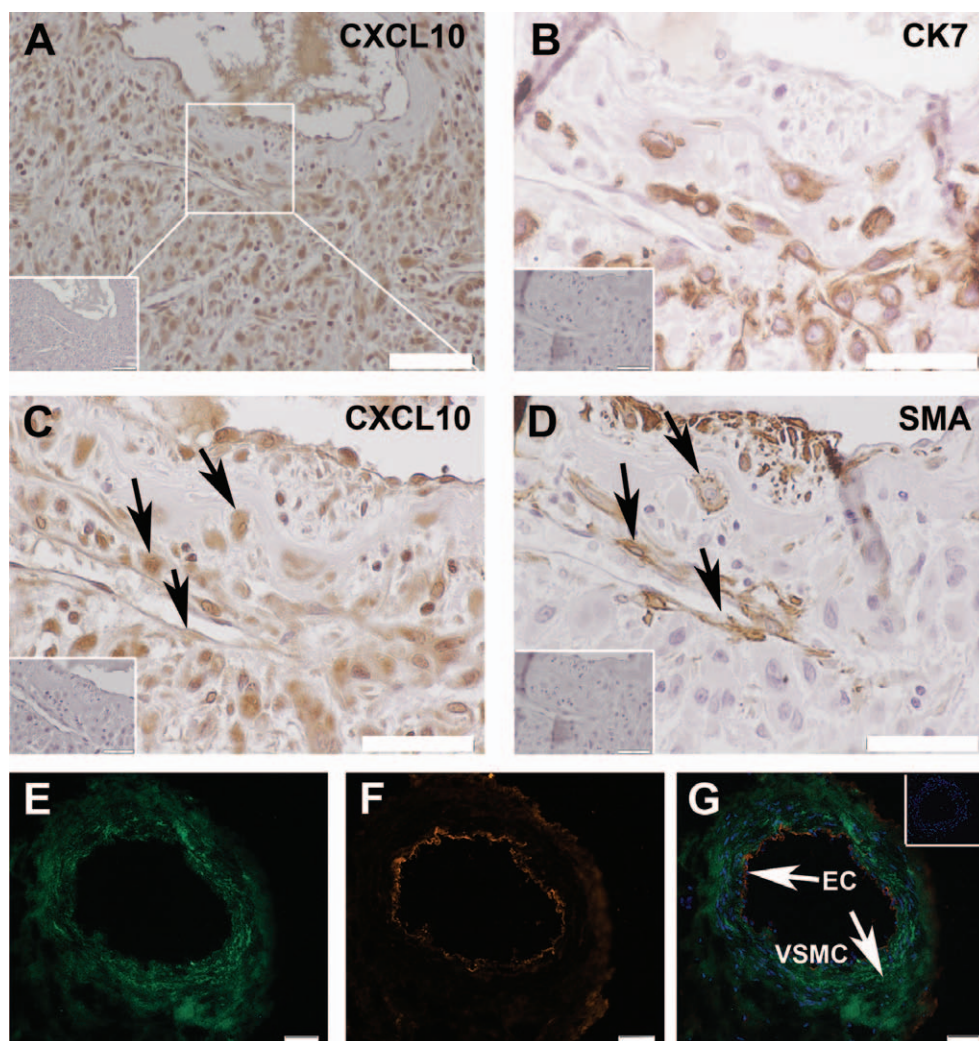


Figure 4. C-X-C motif chemokine 10 (CXCL10) protein is expressed by first trimester decidua and dissected spiral arteries stimulated with trophoblast conditioned media. CXCL10 (**A** and **C**) and α -smooth muscle actin protein (**D**) expression was examined by immunohistochemistry in serially sectioned first trimester decidua ($n=5$; representative image shown). CXCL10 and α -smooth muscle actin protein colocalized to the same cells (indicated by **arrowheads**). Trophoblasts (labeled with CK7, **B**) were present at this stage of remodeling. Negative control (inset) was incubated with nonimmune IgG in place of primary antibody. Scale bar represents 100 μm or 50 μm in zoom. (**E**) Expression of CXCL10 (green) and (**F**) VWF, an endothelial cell marker (red), was examined in a dissected spiral artery treated with extravillous trophoblast (EVT) conditioned media (**G**, merge). EC indicates endothelial cells; and VSM, vascular smooth muscle. Negative control (inset) was incubated with nonimmune IgG in place of primary antibody. Scale bar, 50 μm .

Discussion

Interactions between EC and VSMC are crucial to the stability of a vessel, and physical contact between these cells contributes to the phenotype and differentiation status of both cell types.¹⁹ During decidual SA remodeling in the first trimester of pregnancy, this communication is disrupted and the structural integrity of the vessel is altered. This process is poorly understood because of the difficulties of accessing human implantation sites at this time and the lack of appropriate animal models.⁶ However, understanding the role of fetal trophoblast in the disruption of the stable interactions between cells in the vessel wall of SA is crucial to our understanding of pathologies associated with inadequate vascular remodeling. This study aimed to examine the effect of trophoblast on EC and VSMC interactions using a vascular spheroid 3D coculture model. We determined that trophoblast induce a number of gene expression changes in the

vasculature, including an upregulation of CXCL10, a protein not previously associated with SA remodeling. We examined the expression of CXCL10 in an ex vivo SA model and in first trimester decidual tissue, where it could be localized to α -smooth muscle actin positive cells. Finally, we demonstrated that trophoblast-secreted factors induced dedifferentiation and increased cellular motility of VSMC, a key process in decidual SA remodeling, and that this was, in part, because of CXCL10.

Gene profiling established 101 differentially expressed genes between vascular spheroids cultured with trophoblast CM and control medium. Gene ontology analysis identified that the genes most significantly altered were associated with vascular development. These included the cytokine chemokine (C-C motif) ligand 20 and the protease MMP-10, both of which have been associated with pathological vascular remodeling.^{27,28} MMP-10 degrades collagen type IV and laminin

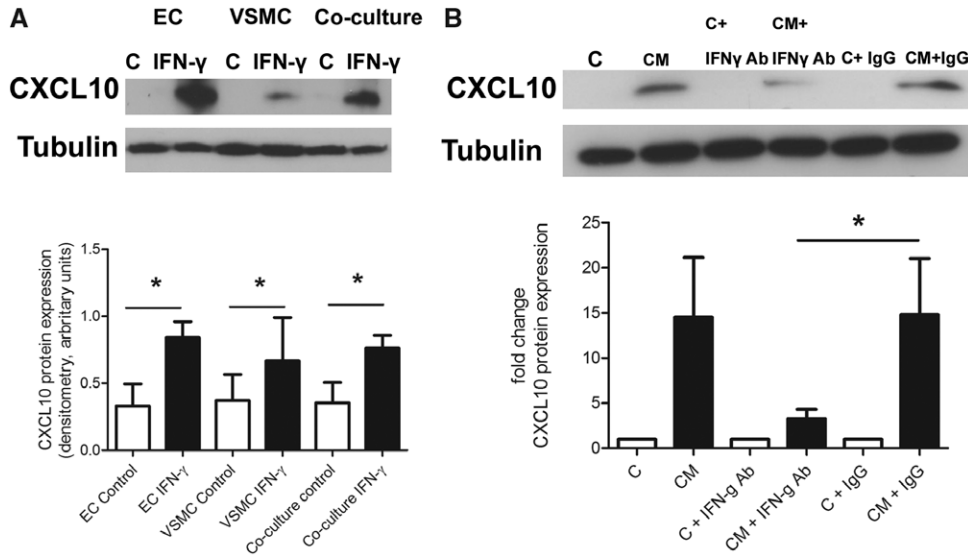


Figure 5. The role of IFN- γ in C-X-C motif chemokine 10 (CXCL10) expression. **A**, Recombinant IFN- γ induces CXCL10 expression in vascular spheroids. Control or rhIFN- γ was added to spheroids made of endothelial cell (EC) alone, vascular smooth muscle cell (VSMC) alone, or cocultured EC/VSMC. CXCL10 expression was measured by Western blot analysis (n=4). **B**, Neutralizing IFN- γ in extravillous trophoblast (EVT) conditioned media (CM) decreased vascular spheroid CXCL10 expression. Control media or EVT CM was incubated with IFN- γ -neutralizing antibody or corresponding IgG control and added to EC/VSMC spheroids. CXCL10 expression was determined by Western blot analysis. * $P < 0.05$ (n=5).

which allows migration of both EC and VSMC. It is capable of stimulating EC motility and tube formation in a mouse angiogenesis plug assay,³¹ and activation of MMP-1, and causes EC network regression by degradation of collagen.³² Also upregulated by trophoblast-secreted factors were the cytokines IL-11 and IL-6, both members of the IL-6-type cytokine family.

IL-6 is expressed in myometrial arteries³³ and is downregulated in VSMC by cell-cell contact with trophoblast, yet can also be upregulated by the secreted factor TNF- α .¹² IL-6 is a proinflammatory cytokine and may affect EVT invasion and cytokine expression.³⁴ The related cytokine IL-11 is associated with implantation and is localized to first trimester decidual EC

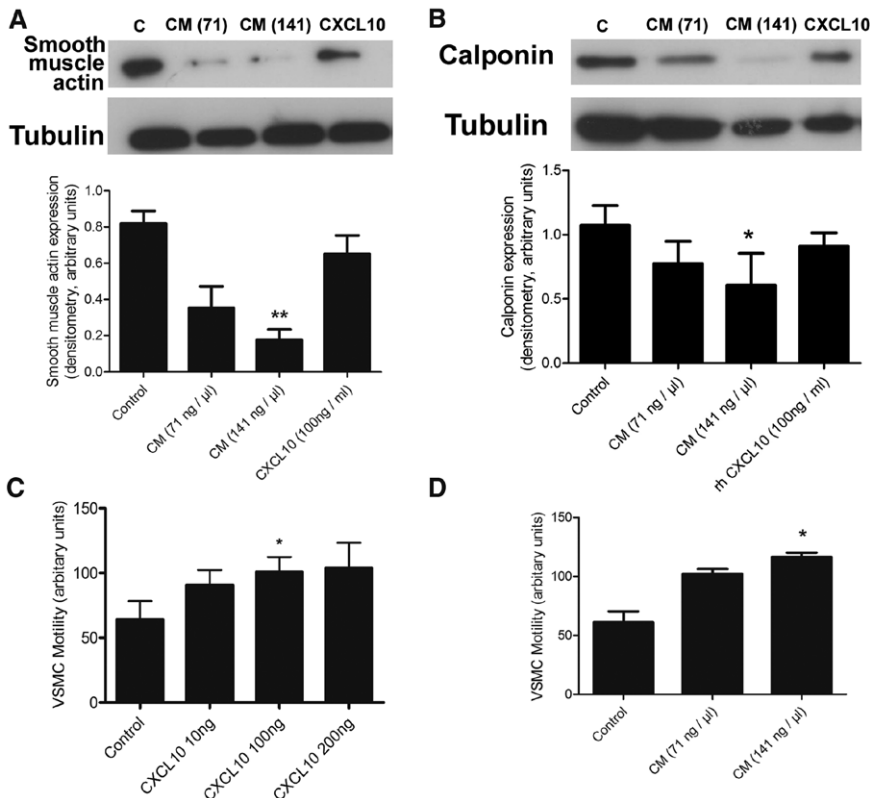


Figure 6. The effects of extravillous trophoblast (EVT) conditioned media (CM) and C-X-C motif chemokine 10 (CXCL10) on vascular smooth muscle cells (VSMCs). VSMCs were incubated for 72 hours in media containing 0.5% FCS, then a further 72 hours with indicated concentrations of EVT CM and recombinant human CXCL10 (n=at least 5 independent experiments). Expression of **(A)** α -smooth muscle actin and **(B)** calponin was examined by Western blot analysis. Time-lapse microscopy was used to analyze the effects of rhCXCL10 **(C)** and EVT CM **(D)** on VSMC motility during a 24-hour incubation. Data are displayed as the mean \pm SEM of a minimum of 3 pooled experiments. * $P < 0.05$; ** $P < 0.01$.

and VSMC, and although its role in these vessels is unknown,³⁵ it has been shown to inhibit VSMC proliferation,³⁶ and as such these 2 related cytokines have the potential for multiple effects in SA remodeling. Similarly, placental growth factor has been associated with apoptosis in vessel remodeling³⁷ and with the regulation of VEGF-dependent remodeling.³⁸ The expression of platelet-derived growth factor-BB that is known to stimulate the dedifferentiation of VSMC³⁹ was increased in response to trophoblast-secreted factors, as were 2 transcription factors, KLF-4 and c-myc, which are implicated in the mediation of this effect.⁴⁰ Therefore, these selected genes, and several others identified by this array, are useful targets that may contribute to the vessel remodeling process by their expression in EC and VSMC in SA.

Expression of the chemokine CXCL10 (previously known as IP-10) was found to be significantly upregulated in vascular spheroids and first trimester SA explants after treatment with EVT CM. It was also expressed by VSMC in the proximity of first trimester SA. However, to our knowledge, this is the first report implicating trophoblast-induced changes in CXCL10 in the physiological remodeling of maternal SA. CXCL10 modulates growth, chemotaxis, and angiogenesis by binding to the CXCR3 receptor⁴¹ and a further unidentified receptor.⁴² It is angiostatic in vitro and in vivo,²⁸ and inhibits both EC proliferation and the induction of apoptosis.^{43,44} CXCL10 and CXCR3 have been associated with vessel remodeling, and are associated with vessel regression in wound repair.²⁸ In support of this, CXCR3 knockout mice exhibit persistent angiogenesis during wound repair.⁴⁵

Regulation of CXCL10 expression by vascular cells is likely to be multifactorial. Major stimuli in a number of cell types, including in uterine microvascular EC,²¹ are proinflammatory cytokines, including IFN- γ . Others have reported that IFN- γ is released by first trimester trophoblast,²⁹ and using a neutralizing antibody, we were able to demonstrate a role for IFN- γ in our study of vascular remodeling. We found enhanced CXCL10 expression in coculture spheroids versus spheroids made up of each individual cell type, indicating that interactions between EC and VSMC are important in the induction of CXCL10. One explanation for this response is that invading trophoblasts secrete bioactive molecules that stimulate EC and VSMC to produce factors that act via paracrine or autocrine mechanisms to enhance the effects of IFN- γ . It is interesting to note that platelet-derived growth factor expression, which is significantly upregulated in the coculture system described above, has been shown to act synergistically with IFN- γ to stimulate CXCL10 expression in other cell systems.⁴⁶

In support of our in vitro findings, we have demonstrated that CXCL10 is expressed in α -smooth muscle actin positive cells in first trimester decidual sections. Interestingly, some cells expressing CXCL10 were found at some distance from the vessel lumen. We therefore investigated the role of both EVT CM and CXCL10 signaling on VSMC and found increased motility, as well as other functional markers of dedifferentiation. Recently, the migration of VSMC from the arteries has been associated with remodeling by trophoblast,⁴⁷ a process unique to remodeling in the decidua. Other mechanisms of disappearance of VSMC during artery remodeling are unknown, however, disruption and disorganization of the VSMC layer has been attributed to both apoptosis and

dedifferentiation.⁴⁸ A decrease in α -smooth muscle actin and calponin expression was observed in VSMC treated with EVT CM, and a small but nonsignificant decrease with rhCXCL10, which indicates a switch to a dedifferentiated, synthetic phenotype.³⁹ A decrease in α -smooth muscle actin expression has been previously demonstrated during SA remodeling, and cells with low expression of α -smooth muscle actin were found at a distance from artery lumens,⁴⁹ similar to the CXCL10-positive cells demonstrated immunohistochemically in our study.

Evidence indicates that trophoblasts synthesize and secrete many factors that could influence the structure of the vessels in both a positive and a negative manner, and that it is the balance between these factors and the way they interact with each other that will determine the extent of remodeling. VSMC have been demonstrated to express CXCR3, the receptor for CXCL10,^{50,51} and, indeed, we demonstrate CXCR3 expression in α -smooth muscle-expressing cells in the decidua. CXCL10 can also signal via a CXCR3-independent mechanism.⁴² As increased proliferation and motility are markers of VSMC dedifferentiation,⁵² autocrine expression and signaling of CXCL10 by VSMC may induce their motility. This has been demonstrated in other cell models, and so therefore may be possible in first trimester decidua.^{53,54} It is also possible that the release of factors such as CXCL10 act as chemokines to recruit interstitial trophoblasts or maternal immune cells, such as decidual natural killer cells, to the remodeling vessel, which are known to influence both EC and VSMC.⁵⁵

In conclusion, we have investigated trophoblast-induced changes in human decidual SA remodeling using a 3D spheroid culture system to model the interactions that occur between the different cell types in vivo.²⁴ We have described the potential of trophoblast-secreted factors, and the resulting increased CXCL10 expression to contribute to SA remodeling during pregnancy by altering the motility and differentiation status of the VSMC compartment of the vessel. Collectively, these results highlight the importance of 3D modeling in examining vascular interactions and provide new insights into the mechanism of SA remodeling.

Acknowledgments

We acknowledge the help of Dr Jayne Dennis (SGUL Medical Biomics Center) in execution of the microarray study, and the staff and patients at the Fetal Medicine Unit, St George's Hospital, for donation of human tissue.

Sources of Funding

This work was supported by St George's University of London and St George's Hospital Fetal Medicine Unit.

Disclosures

None.

References

1. Kam EP, Gardner L, Loke YW, King A. The role of trophoblast in the physiological change in decidual spiral arteries. *Hum Reprod.* 1999;14:2131–2138.
2. Pijnenborg R, Vercruyssen L, Brosens I. Deep placentation. *Best Pract Res Clin Obstet Gynaecol.* 2011;25:273–285.
3. Whitley GS, Cartwright JE. Trophoblast-mediated spiral artery remodeling: a role for apoptosis. *J Anat.* 2009;215:21–26.

4. Zhou Y, Fisher SJ, Janatpour M, Genbacev O, Dejana E, Wheelock M, Damsky CH. Human cytotrophoblasts adopt a vascular phenotype as they differentiate. A strategy for successful endovascular invasion? *J Clin Invest*. 1997;99:2139–2151.
5. Cartwright JE, Fraser R, Leslie K, Wallace AE, James JL. Remodelling at the maternal-fetal interface: relevance to human pregnancy disorders. *Reproduction*. 2010;140:803–813.
6. Carter AM. Animal models of human placentation—a review. *Placenta*. 2007;28:S41–S47.
7. Chen Q, Stone PR, McCowan LM, Chamley LW. Interaction of Jar choriocarcinoma cells with endothelial cell monolayers. *Placenta*. 2005;26:617–625.
8. Cartwright JE, Kenny LC, Dash PR, Crocker IP, Aplin JD, Baker PN, Whitley GS. Trophoblast invasion of spiral arteries: a novel *in vitro* model. *Placenta*. 2002;23:232–235.
9. Xu B, Nakhla S, Makris A, Hennessy A. TNF- α inhibits trophoblast integration into endothelial cellular networks. *Placenta*. 2011;32:241–246.
10. Harris LK, Smith SD, Keogh RJ, Jones RL, Baker PN, Knöfler M, Cartwright JE, Whitley GS, Aplin JD. Trophoblast- and vascular smooth muscle cell-derived MMP-12 mediates elastolysis during uterine spiral artery remodeling. *Am J Pathol*. 2010;177:2103–2115.
11. Aldo PB, Krikun G, Visintin I, Lockwood C, Romero R, Mor G. A novel three-dimensional *in vitro* system to study trophoblast-endothelium cell interactions. *Am J Reprod Immunol*. 2007;58:98–110.
12. Hering L, Herse F, Verlohren S, Park JK, Wellner M, Qadri F, Pijnenborg R, Staff AC, Huppertz B, Muller DN, Luft FC, Dechend R. Trophoblasts reduce the vascular smooth muscle cell proatherogenic response. *Hypertension*. 2008;51:554–559.
13. Wang Y, Lewis DF, Gu Y, Zhang Y, Alexander JS, Granger DN. Placental trophoblast-derived factors diminish endothelial barrier function. *J Clin Endocrinol Metab*. 2004;89:2421–2428.
14. Ashton SV, Whitley GS, Dash PR, Wareing M, Crocker IP, Baker PN, Cartwright JE. Uterine spiral artery remodeling involves endothelial apoptosis induced by extravillous trophoblasts through Fas/FasL interactions. *Arterioscler Thromb Vasc Biol*. 2005;25:102–108.
15. Harris LK, Keogh RJ, Wareing M, Baker PN, Cartwright JE, Aplin JD, Whitley GS. Invasive trophoblasts stimulate vascular smooth muscle cell apoptosis by a fas ligand-dependent mechanism. *Am J Pathol*. 2006;169:1863–1874.
16. Harris LK. IFPA Gabor Than Award lecture: Transformation of the spiral arteries in human pregnancy: key events in the remodelling timeline. *Placenta*. 2011;32 Suppl 2:S154–S158.
17. Whitley GS, Cartwright JE. Cellular and molecular regulation of spiral artery remodelling: lessons from the cardiovascular field. *Placenta*. 2010;31:465–474.
18. Hirschhaeuser F, Menne H, Dittfeld C, West J, Mueller-Klieser W, Kunz-Schughart LA. Multicellular tumor spheroids: an underestimated tool is catching up again. *J Biotechnol*. 2010;148:3–15.
19. Korff T, Kimmina S, Martiny-Baron G, Augustin HG. Blood vessel maturation in a 3-dimensional spheroidal coculture model: direct contact with smooth muscle cells regulates endothelial cell quiescence and abrogates VEGF responsiveness. *FASEB J*. 2001;15:447–457.
20. Eid RE, Rao DA, Zhou J, Lo SF, Ranjbaran H, Gallo A, Sokol SI, Pfau S, Pober JS, Tellides G. Interleukin-17 and interferon-gamma are produced concomitantly by human coronary artery-infiltrating T cells and act synergistically on vascular smooth muscle cells. *Circulation*. 2009;119:1424–1432.
21. Kitaya K, Yasuo T, Yamaguchi T, Fushiki S, Honjo H. Genes regulated by interferon-gamma in human uterine microvascular endothelial cells. *Int J Mol Med*. 2007;20:689–697.
22. Kitaya K, Nakayama T, Daikoku N, Fushiki S, Honjo H. Spatial and temporal expression of ligands for CXCR3 and CXCR4 in human endometrium. *J Clin Endocrinol Metab*. 2004;89:2470–2476.
23. Fickling SA, Holden DP, Cartwright JE, Nussey SS, Vallance P, Whitley GS. Regulation of macrophage nitric oxide synthesis by endothelial cells: a role for NG,NG-dimethylarginine. *Acta Physiol Scand*. 1999;167:145–150.
24. LaMarca HL, Ott CM, Höner Zu Bentrup K, Leblanc CL, Pierson DL, Nelson AB, Scandurro AB, Whitley GS, Nickerson CA, Morris CA. Three-dimensional growth of extravillous cytotrophoblasts promotes differentiation and invasion. *Placenta*. 2005;26:709–720.
25. Korff T, Dandekar G, Pfaff D, Füller T, Goettsch W, Morawietz H, Schaffner F, Augustin HG. Endothelial ephrinB2 is controlled by microenvironmental determinants and associates context-dependently with CD31. *Arterioscler Thromb Vasc Biol*. 2006;26:468–474.
26. Haeger JD, Hambruch N, Dilly M, Froehlich R, Pfarrer C. Formation of bovine placental trophoblast spheroids. *Cells Tissues Organs (Print)*. 2011;193:274–284.
27. Angiolillo AL, Sgadari C, Taub DD, Liao F, Farber JM, Maheshwari S, Kleinman HK, Reaman GH, Tosato G. Human interferon-inducible protein 10 is a potent inhibitor of angiogenesis *in vivo*. *J Exp Med*. 1995;182:155–162.
28. Bodnar RJ, Yates CC, Rodgers ME, Du X, Wells A. IP-10 induces dissociation of newly formed blood vessels. *J Cell Sci*. 2009;122(Pt 12):2064–2077.
29. Murphy SP, Tayade C, Ashkar AA, Hatta K, Zhang J, Croy BA. Interferon gamma in successful pregnancies. *Biol Reprod*. 2009;80:848–859.
30. Wang X, Yue TL, Ohlstein EH, Sung CP, Feuerstein GZ. Interferon-inducible protein-10 involves vascular smooth muscle cell migration, proliferation, and inflammatory response. *J Biol Chem*. 1996;271:24286–24293.
31. Heo SH, Choi YJ, Ryoo HM, Cho JY. Expression profiling of ETS and MMP factors in VEGF-activated endothelial cells: role of MMP-10 in VEGF-induced angiogenesis. *J Cell Physiol*. 2010;224:734–742.
32. Saunders WB, Bayless KJ, Davis GE. MMP-1 activation by serine proteases and MMP-10 induces human capillary tubular network collapse and regression in 3D collagen matrices. *J Cell Sci*. 2005;118:2325–2340.
33. Nilsson LM, Sun ZW, Nilsson J, Nordström I, Chen YW, Molkentin JD, Wide-Swensson D, Hellstrand P, Lydrup ML, Gomez MF. Novel blocker of NFAT activation inhibits IL-6 production in human myometrial arteries and reduces vascular smooth muscle cell proliferation. *Am J Physiol, Cell Physiol*. 2007;292:C1167–C1178.
34. Champion H, Innes BA, Robson SC, Lash GE, Bulmer JN. Effects of interleukin-6 on extravillous trophoblast invasion in early human pregnancy. *Mol Hum Reprod*. 2012;18:391–400.
35. Dimitriadis E, Menkhorst E, Salamonsen LA, Paiva P. Review: LIF and IL11 in trophoblast-endometrial interactions during the establishment of pregnancy. *Placenta*. 2010;31 Suppl:S99–104.
36. Zimmerman MA, Selzman CH, Reznikov LL, Raeburn CD, Barsness K, McIntyre RC Jr, Hamiel CR, Harken AH. Interleukin-11 attenuates human vascular smooth muscle cell proliferation. *Am J Physiol Heart Circ Physiol*. 2002;283:H175–H180.
37. Orlandi A, Ferlosio A, Arcuri G, Scioli MG, De Falco S, Spagnoli LG. Flt-1 expression influences apoptotic susceptibility of vascular smooth muscle cells through the NF-kappaB/IAP-1 pathway. *Cardiovasc Res*. 2010;85:214–223.
38. Andraweera PH, Dekker GA, Roberts CT. The vascular endothelial growth factor family in adverse pregnancy outcomes. *Hum Reprod Update*. 2012;18:436–457.
39. Owens GK, Kumar MS, Wamhoff BR. Molecular regulation of vascular smooth muscle cell differentiation in development and disease. *Physiol Rev*. 2004;84:767–801.
40. Deaton RA, Gan Q, Owens GK. Sp1-dependent activation of KLF4 is required for PDGF-BB-induced phenotypic modulation of smooth muscle. *Am J Physiol Heart Circ Physiol*. 2009;296:H1027–H1037.
41. Weng Y, Siciliano SJ, Waldburger KE, Sirotna-Meisher A, Staruch MJ, Daugherty BL, Gould SL, Springer MS, DeMartino JA. Binding and functional properties of recombinant and endogenous CXCR3 chemokine receptors. *J Biol Chem*. 1998;273:18288–18291.
42. Soejima K, Rollins BJ. A functional IFN-gamma-inducible protein-10/CXCL10-specific receptor expressed by epithelial and endothelial cells that is neither CXCR3 nor glycosaminoglycan. *J Immunol*. 2001;167:6576–6582.
43. Lasagni L, Francalanci M, Annunziato F, Lazzari E, Giannini S, Cosmi L, Sagrafini C, Mazzinghi B, Orlando C, Maggi E, Marra F, Romagnani S, Serio M, Romagnani P. An alternatively spliced variant of CXCR3 mediates the inhibition of endothelial cell growth induced by IP-10, Mig, and I-TAC, and acts as functional receptor for platelet factor 4. *J Exp Med*. 2003;197:1537–1549.
44. Feldman ED, Weinreich DM, Carroll NM, Burness ML, Feldman AL, Turner E, Xu H, Alexander HR Jr. Interferon gamma-inducible protein 10 selectively inhibits proliferation and induces apoptosis in endothelial cells. *Ann Surg Oncol*. 2006;13:125–133.
45. Yates CC, Whaley D, Kulasekaran P, Hancock WW, Lu B, Bodnar R, Newsome J, Hebda PA, Wells A. Delayed and deficient dermal maturation in mice lacking the CXCR3 ELR-negative CXC chemokine receptor. *Am J Pathol*. 2007;171:484–495.
46. Dhillon NK, Peng F, Ransohoff RM, Buch S. PDGF synergistically enhances IFN-gamma-induced expression of CXCL10 in blood-derived macrophages: implications for HIV dementia. *J Immunol*. 2007;179:2722–2730.

47. Bulmer JN, Innes BA, Levey J, Robson SC, Lash GE. The role of vascular smooth muscle cell apoptosis and migration during uterine spiral artery remodeling in normal human pregnancy. *FASEB J*. 2012;26:2975–2985.
48. Smith SD, Dunk CE, Aplin JD, Harris LK, Jones RL. Evidence for immune cell involvement in decidual spiral arteriole remodeling in early human pregnancy. *Am J Pathol*. 2009;174:1959–1971.
49. Hazan AD, Smith SD, Jones RL, Whittle W, Lye SJ, Dunk CE. Vascular-leukocyte interactions: mechanisms of human decidual spiral artery remodeling *in vitro*. *Am J Pathol*. 2010;177:1017–1030.
50. Romagnani P, Annunziato F, Lasagni L, Lazzeri E, Beltrame C, Francalanci M, Uguccioni M, Galli G, Cosmi L, Maurenzig L, Baggiolini M, Maggi E, Romagnani S, Serio M. Cell cycle-dependent expression of CXC chemokine receptor 3 by endothelial cells mediates angiostatic activity. *J Clin Invest*. 2001;107:53–63.
51. Zhao DX, Hu Y, Miller GG, Luster AD, Mitchell RN, Libby P. Differential expression of the IFN-gamma-inducible CXCR3-binding chemokines, IFN-inducible protein 10, monokine induced by IFN, and IFN-inducible T cell alpha chemoattractant in human cardiac allografts: association with cardiac allograft vasculopathy and acute rejection. *J Immunol*. 2002;169:1556–1560.
52. Rensen SS, Doevendans PA, van Eys GJ. Regulation and characteristics of vascular smooth muscle cell phenotypic diversity. *Neth Heart J*. 2007;15:100–108.
53. Laragione T, Brenner M, Sherry B, Gulko PS. CXCL10 and its receptor CXCR3 regulate synovial fibroblast invasion in rheumatoid arthritis. *Arthritis Rheum*. 2011;63:3274–3283.
54. Moriai S, Takahara M, Ogino T, Nagato T, Kishibe K, Ishii H, Katayama A, Shimizu N, Harabuchi Y. Production of interferon- γ -inducible protein-10 and its role as an autocrine invasion factor in nasal natural killer/T-cell lymphoma cells. *Clin Cancer Res*. 2009;15:6771–6779.
55. Fraser R, Whitley GS, Johnstone AP, Host AJ, Sebire NJ, Thilaganathan B, Cartwright JE. Impaired decidual natural killer cell regulation of vascular remodelling in early human pregnancies with high uterine artery resistance. *J Pathol*. 2012;228:322–332.

Supplemental Material

Supplemental Methods

Materials and reagents

L-glutamine, penicillin, streptomycin and endothelial cell growth supplement were obtained from Sigma (Dorset, UK). CXCL10, calponin and tubulin antibodies were purchased from Abcam (Cambridge, UK) and Santa Cruz (Heidelberg, Germany) and Vectashield mounting medium from Vector Labs (Peterborough, UK). CXCL10 recombinant protein was purchased from R & D Systems (Abingdon, UK). Vivaspin columns were purchased from Sartorius Stedim Biotech (Aubagne, France).

Cell culture

The human vascular smooth muscle cell line SGHVSMC-9 (VSMC), derived from transfected human aortic vascular smooth muscle cells, was maintained as previously described¹ in Ham's F10 medium (Invitrogen Life Technologies, Paisley, UK) supplemented with 10% (v/v) fetal bovine serum (FBS), L-glutamine (2 mmol/L), penicillin (100 IU/ml), and streptomycin (100 µg/ml). This cell line has been well characterised for use in these studies^{2, 3}. The human endothelial cell line SGHEC-7 was maintained as previously described⁴ in Medium 199 supplemented with Earle's modified salts (M199; GIBCO Invitrogen, UK): RPMI 1640 (Sigma, UK) medium in a ratio of 1:1 containing L-glutamine (2 mmol/L), penicillin (100 IU/ml), streptomycin (100 µg/ml), gentamicin (16mg/ml), supplemented with endothelial cell growth supplement (ECGS, 2.5 µg/ml) and 10% (v/v) FBS. The well characterised human extravillous trophoblast (EVT) cell line SGHPL-4 was derived from primary human first trimester EVT⁵. SGHPL-4 cells were cultured in Hams F10 media supplemented with 10% (v/v) FBS, containing L-glutamine (2 mmol/L), penicillin (100 IU/ml), and streptomycin (100 µg/ml). All cells were incubated with 95% air and 5% carbon dioxide at 37°C in a humidified incubator.

Generation of EVT conditioned media

SGHPL-4 cells were grown in 3-dimensional culture as previously described⁶. Briefly, 4×10^6 cells were added to 25ml Universal tubes containing 20mg of gelatin-coated Cytodex-3 microcarrier beads (Sigma) and cultured on a spiralex roller at 37°C in phenol-red-free RPMI-1640 (GIBCO) containing 10% (v/v) FCS and 25mM Hepes buffer. After 24 h the medium was removed and the cells and beads washed twice with PBS. Medium was then replaced with phenol-red-free RPMI-1640 containing 25mM Hepes. Conditioned medium (CM) was collected after 48 h, spun at 5000g through a Vivaspin 20 (3000 mwco PES) column at 4°C. The concentrated media was then made up to x1 with phenol-red-free RPMI-1640 and this centrifugation step repeated. The protein concentration of the resulting concentrated CM was determined by Bradford assay and stored at -20°C at a final concentration of 0.5µg/µl. IFN-γ was neutralised in CM by 1 hour pre-incubation with mouse anti-human IFN-γ (0.3 µg/ml, R&D systems, MAB2852) or control mouse IgG (0.3 µg/ml, Sigma) before use in experiments.

Spheroid generation and treatments

To generate spheroids, a hanging drop culture method was used^{7, 8}. VSMC and SGHEC-7 were cultured alone or in co-culture in equal numbers in VSMC media containing 0.5% (v/v) FBS and 25% (v/v) carboxymethylcellulose and 30 µl containing a total of 1500 cells (co-culture: 750 VSMC and 750 SGHEC-7) was placed on the underside of a petri dish lid. Spheroids were left to form for 24 hours before use in experiments. The following treatments were added to the spheroids for 24 hours: EVT CM at a concentration of 71 ng / µl, rhIFN-γ (500 U/ml, R&D systems), IFN-γ neutralised CM as above. Phenol-red free RPMI 1640 media was added to spheroids as a control. At the end of the incubation period, spheroids

(n=64) were collected, pooled, and washed 3 x in PBS. Spheroids were then lysed for microarray, RNA isolation or protein isolation, or fixed in 4% (w/v) paraformaldehyde in PBS for immunohistochemical analysis.

RNA isolation

RNA was extracted using RNEasy mini kit according to manufacturer's instructions (Qiagen, West Sussex, UK).

Microarray analysis

RNA was reverse transcribed into cDNA, amplified and transcribed into cRNA using the Illumina TotalPrep RNA amplification kit (Ambion, Life Technologies, Warrington, UK) according to manufacturer's instructions. The cRNA was then assessed for quantity and quality by Agilent RNA 6000 Pico Kit (Agilent Technologies, Germany) and NanoDrop (ThermoScientific, West Sussex, UK) and hybridised to Illumina Sentrix BeadChip Array Human HT-12_v4_Beadchip (Illumina) according to manufacturer's instructions, and scanned on an Illumina GX500 Beadstation. Idat files were imported to GenomeStudio (Illumina) and raw data exported in text format. Data comparing spheroids treated with trophoblast conditioned or control media was analysed in GeneSpring v11.5.1 (Agilent Technologies). In brief data was normalised using quantile normalisation and baseline transformed to the median of all control samples. Sample distributions were checked for consistency and conformity to a gaussian distribution by qualitative methods and replicate consistency was assessed using principal component analysis. Data was filtered to remove unexpressed or unreliable data such that remaining entities should have a detection p-value of greater than 0.6 in 100% of samples for any one of the two conditions and a fold change of greater than 1.5 compared to the control. An unpaired t-test was performed in conjunction with a Benjamini-Hochberg multiple testing correction and a corrected p-value of <0.05 was applied. GO analysis was performed using a corrected p-value of <0.05. Microarray data are available in the ArrayExpress database (www.ebi.ac.uk/arrayexpress) under accession number E-MTAB-1462.

SYBR green quantitative RT-PCR analysis

Spheroid RNA samples (64 spheroids per experiment, n=3) were reverse transcribed using Bioline cDNA Synthesis kit according to manufacturer's instructions (Bioline, London, UK). 40ng of cDNA was used in duplicate samples for quantitative RT-PCR using Power SYBR green Master Mix (Applied Biosystems, Life Technologies) as manufacturer's instructions using the following sequence specific primers:

18S: ACA-CGT-TCC-ACC-TCA-TCC-TC and CTT-TGC-CAT-CAC-TGC-CAT-TA
 CXCL10: TTC-AAG-GAG-TAC-CTC-TCT-CTA-G and CTG-GAT-TCA-GAC-ATC-TCT-TCT-C
 STC-1: CAG-GCT-TCG-GAC-AAG-TCT-GT and ACA-GCA-AGC-TGA-ATG-TGT-GC
 PGF - GTC-TCC-TCC-TTT-CCG-GCT-T and TGC-AGC-TCC-TAA-AGA-TCC-GTT

Q-PCR was carried out using a Bio-Rad CFX96 Real-Time PCR Detection System (Bio-Rad, Hemel Hempstead, UK). Expression of analysed genes was normalised to RNA loading for each sample using the 18S ribosomal RNA as an internal standard.

Western Blot Analysis

Protein was resolved on 8–10% sodium dodecyl sulphate (SDS)–polyacrylamide gels before transfer onto Hybond P membrane (Amersham, UK). Non-specific reactivity was blocked with 5% (w/v) non-fat dried milk in Tris-buffered saline containing 0.1% (v/v) Tween-20 (TBST) for 1 h at room temperature. Blots were incubated overnight at 4°C with rabbit anti CXCL10 (0.5 µg/ml, Abcam ab9807), mouse anti α -smooth muscle actin (0.1 µg/ml, Dako, clone 1A4) or rabbit anti-calponin (1:1000, Abcam ab46794). Peroxidase conjugated secondary antibodies (1:10000, Sigma) were incubated at room temperature for 1 h and detection was performed using ECL Plus (Millipore, Watford, UK). Blots were subsequently blocked and re-probed with a mouse anti tubulin antibody (0.15 µg/ml, Abcam, ab11323).

Western blots were scanned and the integrated intensity of each band determined using ImageJ version 1.43u. Western blots shown are representative of at least three separate experiments and expressed as a ratio to tubulin in the same sample.

***Ex vivo* vessel explant model**

Informed consent was obtained and ethical committee approval was in place for all studies. Decidual/myometrial biopsies (n=3) were obtained from pregnant women undergoing elective Caesarean section at term for reasons such as breech presentation. These were taken from non-placental bed areas from the upper leaf of the lower segment Caesarean incision. In event of a placenta low-lying in the lower segment, uterine biopsies were likely to be from placental bed and so were not taken because of the risk of maternal post-partum haemorrhage. Spiral arteries were dissected as previously described⁹ using a stereo microscope with minimal surrounding tissue. Vessels were incubated in individual wells of a 96 well plate with EVT conditioned media for 24 hours, before being snap-frozen and cryosectioned for immunohistochemical staining.

Immunohistochemistry

Spiral artery immunohistochemistry

Sections were fixed in 4% (w/v) paraformaldehyde in PBS for 10 minutes, washed in PBS, and permeabilized in 0.2% (v/v) Triton X-100 in PBS for 5 minutes. After 3 washes with PBS, blocking buffer (PBS in 10% (v/v) goat serum) was added for 30 minutes, then sections were incubated in mouse anti-human CXCL10 antibody (2 µg/ml, Santa Cruz, sc101500), or isotype control immunoglobulin overnight at 4°C. After 3 washes, sections were incubated for 30 minutes with biotinylated goat anti-mouse (7.5 µg/ml, Vector Laboratories). After 3 further washes, sections were incubated with fluorescein-streptavidin (15 µg/mL, Vector Laboratories) for 45 minutes. Sections were then re-blocked in normal goat serum and rabbit anti-VWF antibody (17.1 µg/ml, Dako, UK) was added for 1 hour at room temperature. Sections were then incubated with goat anti-rabbit Alexafluor 546 (Molecular probes, Invitrogen, UK) for 45 minutes, washed extensively, and mounted using Vectashield mounting medium with DAPI to visualise nuclei.

Spheroid immunohistochemistry

Spheroids were washed with PBS and fixed in 4% (w/v) paraformaldehyde in PBS for 10 minutes and then washed in fixative buffer (30% (w/v) sucrose, 90mM MgCl₂ in 2X PBS). Spheroids were then suspended in a small volume of 1.5% (w/v) agarose/5% (w/v) sucrose in PBS which was allowed to set. The resultant blocks were placed in a 30% (w/v) sucrose in water solution until each block had sunk. Blocks were then frozen on dry ice and cryosectioned in 15 µm sections through roughly the centre of the spheroid. Spheroid sections were then immunostained as spiral artery sections.

Decidual immunohistochemistry

Products of conception were obtained from women attending clinic for elective termination of pregnancy between 9-12 weeks. Research Ethics Committee approval was in place and all women gave informed written consent. Decidual fragments were fixed in formalin, paraffin embedded and 10µm sections cut.

Slides were dewaxed in xylene for 10 minutes followed by rehydration through graded ethanol (100%, 95%, 80%, and 70%) for 20 seconds each and a final wash in water. Antigen retrieval was performed in boiling citrate buffer (0.01M, pH 6) for 5 minutes and left to stand for a further 20 minutes. Endogenous peroxidase activity was then blocked by washing sections in 3% (v/v) hydrogen peroxide in methanol. After a brief wash in tap water slides were washed in Tris buffered saline (TBS, pH 7.5) twice for 5 minutes each. Sections were then incubated in 10% normal goat serum for at least 30 minutes at room temperature. Mouse anti-human CXCL10 antibody (2 µg/ml, Santa Cruz), mouse anti-human smooth

muscle actin antibody (0.2 µg/ml Dako, UK clone 1A4), mouse anti-cytokeratin 7 antibody (3.1 µg/ml, DAKO clone OV-TL 12/30) or mouse anti-CXCR3 antibody (3.3 µg/ml, Abcam ab64714) was then applied and incubated at 4 °C overnight. Control sections were included with non-immune IgG. Following further washes in TBS, the biotinylated and horseradish peroxidase-conjugated secondary antibody was applied for 10 minutes at room temperature (Histofine kit, Invitrogen, UK). Sections were incubated with DAB (DAKO, UK) for 1-5 minutes until positive staining was identified by a brown colour under x10 magnification. Sections were then counterstained for 1-5 minutes in haematoxylin, mounted and visualised.

Confocal microscopy

For confocal analysis, before co-culture and spheroid generation cells were incubated for 30 minutes at 37°C with 1 nM CellTracker™ Green or Orange (Molecular Probes, Invitrogen, UK). Spheroids were then mounted in 80% (v/v) glycerol on a concave slide. The spheroids were analysed using a confocal laser scanning microscope (CLSM) with an LSM 510 Meta inverted microscope (Zeiss, Hertfordshire, UK) and the LSM 510 image examiner software (Zeiss).

Time-lapse microscopy

Motility of VSMC was observed over time using an Olympus IX70 inverted microscope equipped with a Hamamatsu C4742-95 digital camera. VSMC were incubated in medium containing 0.5% (v/v) FBS for 24 h, at which point they were transferred to the microscope chamber in fresh medium containing vehicle (PBS) or indicated concentrations of CXCL10 or conditioned media. The microscope and stage were enclosed within a heated (37°C) chamber (Solent Scientific, UK) and cells were cultured in 5% CO₂ in air. Images were captured every 15 min for 24 hours and analysed using Image Pro Plus software (Media Cybernetics, USA). For analysis, 20 cells in 2 fields of view for each treatment were chosen at random at the beginning of the time-lapse sequence and the distance moved by each cell recorded.

1. Keogh RJ, Harris LK, Freeman A, Baker PN, Aplin JD, Whitley GS, Cartwright JE. Fetal-derived trophoblast use the apoptotic cytokine tumor necrosis factor-alpha-related apoptosis-inducing ligand to induce smooth muscle cell death. *Circ Res*. 2007;100:834-841
2. Harris LK, Baker PN, Keogh RJ, Cartwright JE, Whitley GS, Aplin JD. Trophoblast-induced smooth muscle cell apoptosis during spiral artery remodelling involves fas/fas ligand interactions. *Placenta*. 2005;26:A.77 (Abstract)
3. Harris LK, Keogh RJ, Wareing M, Baker PN, Cartwright JE, Aplin JD, Whitley GS. Invasive trophoblasts stimulate vascular smooth muscle cell apoptosis by a fas ligand-dependent mechanism. *Am J Pathol*. 2006;169:1863-1874
4. Fickling SA, Holden DP, Cartwright JE, Nussey SS, Vallance P, Whitley GS. Regulation of macrophage nitric oxide synthesis by endothelial cells: A role for ng,ng-dimethylarginine. *Acta Physiol Scand*. 1999;167:145-150
5. Cartwright JE, Holden DP, Whitley GS. Hepatocyte growth factor regulates human trophoblast motility and invasion: A role for nitric oxide. *Br J Pharmacol*. 1999;128:181-189
6. LaMarca HL, Ott CM, Honer Zu Bentrup K, Leblanc CL, Pierson DL, Nelson AB, Scandurro AB, Whitley GS, Nickerson CA, Morris CA. Three-dimensional growth of extravillous cytotrophoblasts promotes differentiation and invasion. *Placenta*. 2005;26:709-720
7. Korff T, Dandekar G, Pfaff D, Fuller T, Goetsch W, Morawietz H, Schaffner F, Augustin HG. Endothelial ephrinb2 is controlled by microenvironmental determinants and associates context-dependently with cd31. *Arterioscler Thromb Vasc Biol*. 2006;26:468-474
8. Haeger JD, Hambruch N, Dilly M, Froehlich R, Pfarrer C. Formation of bovine placental trophoblast spheroids. *Cells Tissues Organs*. 2011;193:274-284
9. Cartwright JE, Kenny LC, Dash PR, Crocker IP, Aplin JD, Baker PN, Whitley GS. Trophoblast invasion of spiral arteries: A novel in vitro model. *Placenta*. 2002;23:232-235

Supplemental Tables

Supplemental Table I: Vascular spheroid gene expression altered over 1.5 fold by trophoblast conditioned media

Gene Name / Symbol	Fold change absolute	Corrected p-value	Up / down
Homo sapiens CD93 molecule (CD93), mRNA.	2.594932	0.006259621	up
Homo sapiens stanniocalcin 1 (STC1), mRNA.	2.340758	0.001881272	up
Homo sapiens chemokine (C-C motif) ligand 20 (CCL20), mRNA.	2.278803	0.037411097	up
Homo sapiens podocalyxin-like (PODXL), transcript variant 1, mRNA.	2.276604	0.011221726	up
Homo sapiens chemokine (C-X-C motif) ligand 10 (CXCL10), mRNA.	2.241451	0.020344842	up
Homo sapiens interleukin 6 (interferon, beta 2) (IL6), mRNA.	2.208562	0.02667893	up
Homo sapiens tissue factor pathway inhibitor 2 (TFPI2), mRNA.	2.202464	0.015408089	up
Homo sapiens transmembrane protein 158 (TMEM158), mRNA.	2.152755	0.006259621	up
Homo sapiens interleukin 11 (IL11), mRNA.	2.143356	0.008667579	up
Homo sapiens placental growth factor (PGF), mRNA.	2.018083	0.015408089	up
Homo sapiens hedgehog interacting protein (HHIP), mRNA.	1.998893	0.017495126	up
Homo sapiens interleukin 8 (IL8), mRNA.	1.943614	0.020018023	up
Homo sapiens chemokine (C-X-C motif) receptor 4 (CXCR4), transcript variant 2, mRNA.	1.935163	0.008772412	up
Homo sapiens podocalyxin-like (PODXL), transcript variant 1, mRNA.	1.925909	0.008772412	up
Homo sapiens prostaglandin-endoperoxide synthase 2 (prostaglandin G/H synthase and cyclooxygenase) (PTGS2), mRNA.	1.875883	0.027641652	up
Homo sapiens secretogranin V (7B2 protein) (SCG5), mRNA.	1.871887	0.001881272	up
Homo sapiens coagulation factor II (thrombin) receptor-like 1 (F2RL1), mRNA.	1.870356	0.012442495	up
Homo sapiens matrix metalloproteinase 10 (stromelysin 2) (MMP10), mRNA.	1.859341	0.037411097	up
Homo sapiens serum/glucocorticoid regulated kinase 1 (SGK1), transcript variant 1, mRNA.	1.8578	0.020344842	up
Homo sapiens serum/glucocorticoid regulated kinase (SGK), mRNA.	1.838739	0.02667893	up
Homo sapiens KIAA1199 (KIAA1199), mRNA.	1.825166	0.032360554	up
Homo sapiens tumor necrosis factor, alpha-induced protein 6 (TNFAIP6), mRNA.	1.79597	0.023012258	up
Homo sapiens solute carrier family 25 (mitochondrial carrier; phosphate carrier), member 24 (SLC25A24), nuclear gene encoding mitochondrial protein, transcript variant 1, mRNA.	1.774163	0.036931	up
Homo sapiens dishevelled associated activator of morphogenesis 1 (DAAM1), mRNA.	1.773732	0.017495126	up
Homo sapiens neurotrimin (NTM), transcript variant 2, mRNA.	1.766954	0.006259621	up
Homo sapiens phosphodiesterase 4B, cAMP-specific (phosphodiesterase E4 dunce homolog, Drosophila) (PDE4B), transcript variant a, mRNA.	1.757134	0.019516693	up
Homo sapiens NADPH oxidase 4 (NOX4), mRNA.	1.755237	0.008667579	up
Homo sapiens coagulation factor II (thrombin) receptor-like 1 (F2RL1), mRNA.	1.746881	0.028023487	up
Homo sapiens collagen, type VI, alpha 3 (COL6A3), transcript variant 3, mRNA.	1.736037	0.021656875	up

Homo sapiens gremlin 1, cysteine knot superfamily, homolog (<i>Xenopus laevis</i>) (GREM1), mRNA.	1.708331	0.042738255	up
Homo sapiens serpin peptidase inhibitor, clade B (ovalbumin), member 2 (SERPINB2), mRNA.	1.704612	0.030201832	up
Homo sapiens regulator of G-protein signalling 4 (RGS4), mRNA.	1.702098	0.042020477	up
Homo sapiens collagen, type VI, alpha 3 (COL6A3), transcript variant 1, mRNA.	1.696903	0.02667893	up
Homo sapiens dual specificity phosphatase 6 (DUSP6), transcript variant 2, mRNA.	1.688827	0.021656875	up
Homo sapiens SRY (sex determining region Y)-box 18 (SOX18), mRNA.	1.684359	0.017021826	up
Homo sapiens cadherin 5, type 2, VE-cadherin (vascular epithelium) (CDH5), mRNA.	1.683726	0.02667893	up
Homo sapiens endothelial cell-specific molecule 1 (ESM1), mRNA.	1.680873	0.037411097	up
Homo sapiens serum/glucocorticoid regulated kinase 1 (SGK1), transcript variant 1, mRNA.	1.664353	0.024545638	up
Homo sapiens platelet-derived growth factor beta polypeptide (simian sarcoma viral (v-sis) oncogene homolog) (PDGFB), transcript variant 1, mRNA.	1.661473	0.02667893	up
Homo sapiens prostate transmembrane protein, androgen induced 1 (PMEPA1), transcript variant 2, mRNA.	1.652479	0.031239437	up
PREDICTED: Homo sapiens hypothetical protein LOC440345, transcript variant 6 (LOC440345), mRNA.	1.652412	0.006259621	down
Homo sapiens dual specificity phosphatase 6 (DUSP6), transcript variant 1, mRNA.	1.65127	0.021656875	up
Homo sapiens septin 4 (SEPT4), transcript variant 2, mRNA.	1.649398	0.047301278	down
Homo sapiens growth arrest-specific 1 (GAS1), mRNA.	1.648486	0.022904437	up
Homo sapiens nuclear receptor subfamily 4, group A, member 2 (NR4A2), transcript variant 1, mRNA.	1.645724	0.023800679	up
Homo sapiens guanylate binding protein 1, interferon-inducible, 67kDa (GBP1), mRNA.	1.641342	0.020344842	up
Homo sapiens thrombomodulin (THBD), mRNA.	1.639041	0.017021826	up
Homo sapiens protein tyrosine phosphatase, receptor type, E (PTPRE), transcript variant 2, mRNA.	1.637211	0.025211982	up
Homo sapiens endothelial cell-specific molecule 1 (ESM1), mRNA.	1.633846	0.03043533	up
Homo sapiens cyclin D1 (CCND1), mRNA.	1.631296	0.015408089	up
Homo sapiens LFNG O-fucosylpeptide 3-beta-N-acetylglucosaminyltransferase (LFNG), transcript variant 1, mRNA.	1.629187	6.67E-04	up
Homo sapiens plexin A2 (PLXNA2), mRNA.	1.626524	0.008667579	up
Homo sapiens HECT, C2 and WW domain containing E3 ubiquitin protein ligase 2 (HECW2), mRNA.	1.626333	0.015408089	up
Homo sapiens EGF, latrophilin and seven transmembrane domain containing 1 (ELTD1), mRNA.	1.625174	0.015408089	up
Homo sapiens prostate transmembrane protein, androgen induced 1 (PMEPA1), transcript variant 2, mRNA.	1.624929	0.015408089	up
Homo sapiens adenomatous polyposis coli down-regulated 1-like (APCDD1L), mRNA.	1.617783	0.022904437	up
Homo sapiens endothelial differentiation, sphingolipid G-protein-coupled receptor, 1 (EDG1), mRNA.	1.613336	0.028148912	up
Homo sapiens chromosome 4 open reading frame 49 (C4orf49), mRNA.	1.596915	0.022904437	down
Homo sapiens tribbles homolog 1 (<i>Drosophila</i>) (TRIB1), mRNA.	1.587401	0.02667893	up
Homo sapiens cathepsin C (CTSC), transcript variant 1, mRNA.	1.581769	0.001881272	up
Homo sapiens 5'-nucleotidase, ecto (CD73) (NT5E), mRNA.	1.581389	0.017495126	up

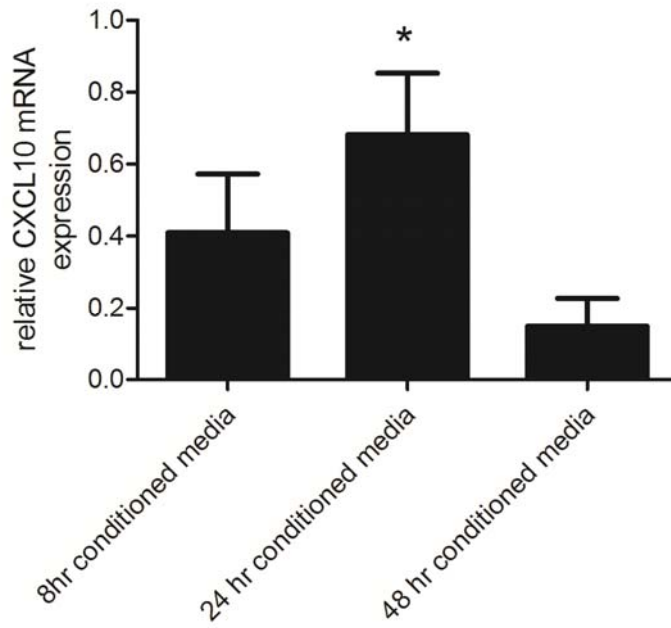
Homo sapiens potassium voltage-gated channel, shaker-related subfamily, beta member 1 (KCNA1), transcript variant 2, mRNA.	1.579729	0.018453117	up
Homo sapiens platelet-derived growth factor beta polypeptide (simian sarcoma viral (v-sis) oncogene homolog) (PDGFB), transcript variant 2, mRNA.	1.575343	0.022904437	up
Homo sapiens glutamine-fructose-6-phosphate transaminase 2 (GFPT2), mRNA.	1.571108	0.022904437	up
Homo sapiens pleckstrin 2 (PLEK2), mRNA.	1.568859	0.012779525	up
Homo sapiens lipase, endothelial (LIPG), mRNA.	1.568142	0.019516693	up
Homo sapiens SH2 domain containing 3C (SH2D3C), transcript variant 2, mRNA.	1.567942	0.023925005	up
Homo sapiens dehydrogenase/reductase (SDR family) member 3 (DHRS3), mRNA.	1.56785	0.011221726	down
Homo sapiens Epstein-Barr virus induced gene 2 (lymphocyte-specific G protein-coupled receptor) (EBI2), mRNA.	1.566772	0.022904437	up
Homo sapiens protein tyrosine phosphatase, receptor type, E (PTPRE), transcript variant 2, mRNA.	1.566606	0.02086765	up
Homo sapiens heparin-binding EGF-like growth factor (HBEGF), mRNA.	1.565329	0.02667893	up
Homo sapiens v-myc myelocytomatosis viral oncogene homolog (avian) (MYC), mRNA.	1.563026	0.02667893	up
Homo sapiens serpin peptidase inhibitor, clade E (nexin, plasminogen activator inhibitor type 1), member 2 (SERPINE2), mRNA.	1.561675	0.009054425	up
Homo sapiens interleukin 1, alpha (IL1A), mRNA.	1.559357	0.020344842	up
Homo sapiens glutathione peroxidase 3 (plasma) (GPX3), mRNA.	1.558923	0.017021826	down
Homo sapiens small Cajal body-specific RNA 14 (SCARNA14), guide RNA.	1.555441	0.03776642	up
Homo sapiens protein kinase (cAMP-dependent, catalytic) inhibitor alpha (PKIA), transcript variant 7, mRNA.	1.554495	0.017021826	up
Homo sapiens protein kinase (cAMP-dependent, catalytic) inhibitor alpha (PKIA), transcript variant 6, mRNA.	1.551958	0.020344842	up
Homo sapiens cleavage stimulation factor, 3' pre-RNA, subunit 3, 77kDa (CSTF3), transcript variant 3, mRNA.	1.551671	0.017021826	down
Homo sapiens wingless-type MMTV integration site family, member 5A (WNT5A), mRNA.	1.548196	0.037411097	up
Homo sapiens MAM domain containing 2 (MAMDC2), mRNA.	1.544279	0.008667579	up
Homo sapiens CD44 molecule (Indian blood group) (CD44), transcript variant 4, mRNA.	1.540968	0.02667893	up
Homo sapiens hypothetical LOC100216001 (LOC100216001), non-coding RNA.	1.538554	0.008772412	up
Homo sapiens transmembrane protein 200A (TMEM200A), mRNA.	1.537259	0.017021826	up
Homo sapiens latent transforming growth factor beta binding protein 2 (LTBP2), mRNA.	1.536061	0.008667579	up
Homo sapiens phosphodiesterase 4B, cAMP-specific (phosphodiesterase E4 dunce homolog, Drosophila) (PDE4B), transcript variant a, mRNA.	1.535905	0.02667893	up
Homo sapiens phosphodiesterase 7B (PDE7B), mRNA.	1.534708	0.008667579	up
Homo sapiens sphingosine-1-phosphate receptor 1 (S1PR1), mRNA.	1.529714	0.022904437	up
Homo sapiens chemokine (C-X-C motif) receptor 4 (CXCR4), transcript variant 1, mRNA.	1.529364	0.017021826	up
Homo sapiens OCIA domain containing 2 (OCIAD2), transcript variant 2, mRNA.	1.526341	0.011221726	up
Homo sapiens mRNA; cDNA DKFZp762M127 (from clone DKFZp762M127)	1.525293	0.028023487	up
Homo sapiens nucleolar protein 12 (NOL12), mRNA.	1.519159	0.03043533	down

Homo sapiens chromosome 4 open reading frame 18 (C4orf18), transcript variant 2, mRNA.	1.514323	0.017021826	up
Homo sapiens pterin-4 alpha-carbinolamine dehydratase/dimerization cofactor of hepatocyte nuclear factor 1 alpha (PCBD1), mRNA.	1.511084	0.015408089	down
Homo sapiens sushi-repeat-containing protein, X-linked 2 (SRPX2), mRNA.	1.510306	0.017495126	up
Homo sapiens Parkinson disease 7 domain containing 1 (PDDC1), mRNA.	1.508039	0.02171086	down
Homo sapiens hypothetical locus LOC401237 (FLJ22536), non-coding RNA.	1.506264	0.007810248	up
Homo sapiens sushi-repeat-containing protein, X-linked (SRPX), mRNA.	1.505457	0.017021826	up
Homo sapiens hyaluronoglucosaminidase 2 (HYAL2), transcript variant 1, mRNA.	1.505197	0.022904437	up
full-length cDNA clone CS0DA009YB08 of Neuroblastoma of Homo sapiens (human)	1.502986	0.02667893	up
Homo sapiens Kruppel-like factor 4 (gut) (KLF4), mRNA.	1.502778	0.020344842	up

Supplemental Table II: Full list of gene ontologies of vascular spheroid gene expression altered over 1.5 fold by trophoblast conditioned media

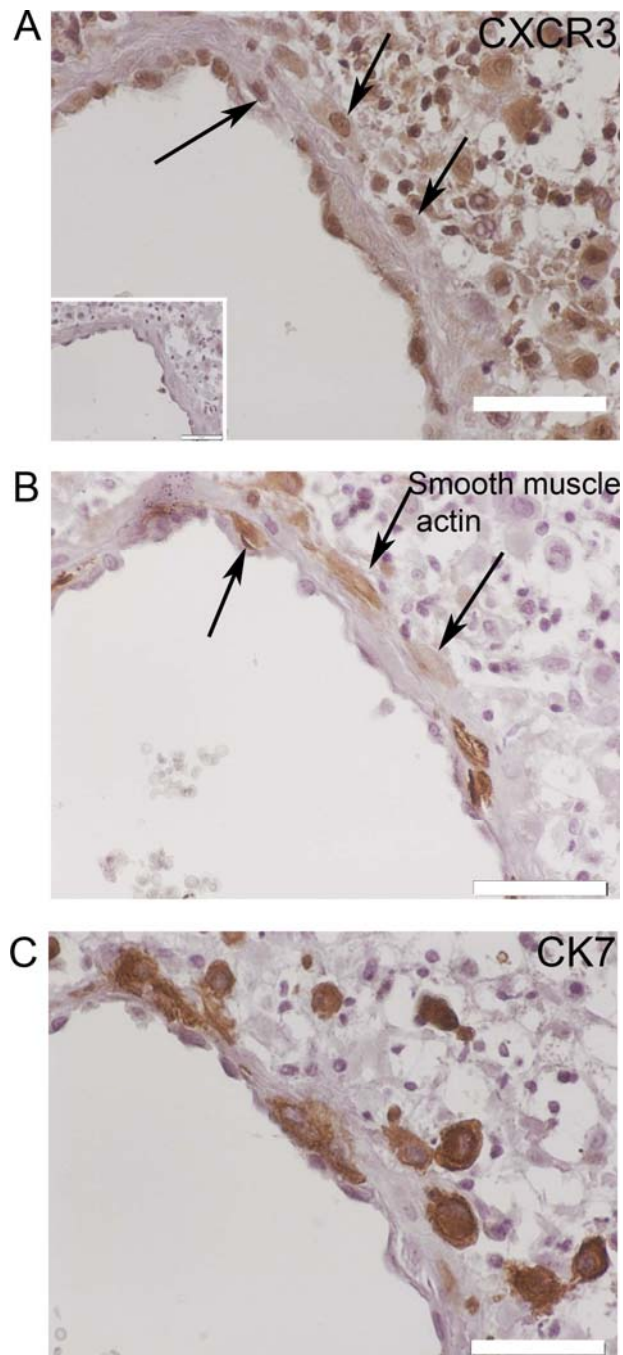
Biological Process	Number of genes	P value
Regulation of cell proliferation	16	9.08E-05
Response to wounding	15	9.08E-05
Response to external stimulus	17	3.92E-04
Response to stress	23	1.00E-03
Organ morphogenesis	11	7.00E-03
Regulation of locomotion	8	7.00E-03
Organ development	20	9.00E-03
Regulation of phosphorylation	12	0.009
Regulation of phosphorus metabolic process	13	1.10E-02
Regulation of phosphate metabolic process	13	1.10E-02
Cell-cell signaling	11	1.10E-02
Negative regulation of cell proliferation	8	1.20E-02
Signal transduction	37	0.014
Cell communication	39	0.014
Positive regulation of cell proliferation	9	0.014
Inflammatory response	9	0.017
Anatomical structure morphogenesis	14	0.022
Regulation of cell migration	6	0.022
Regulation of localization	10	0.031
Regulation of cellular component movement	6	0.033
Angiogenesis	5	0.033
Blood vessel development	6	0.033
Vasculature development	6	0.036
Regulation of protein kinase activity	9	0.036
Regulation of map kinase activity	6	0.036
Anatomical structure development	23	0.036
System development	22	0.037
Regulation of kinase activity	9	0.037

Regulation of transferase activity	9	0.041
Negative regulation of protein kinase activity	4	0.043
Positive regulation of peptidyl serine phosphorylation	2	0.043
Regulation of peptidyl serine phosphorylation	2	0.043
Negative regulation of kinase activity	4	0.043
Biological regulation	54	0.043
Response to stimulus	27	0.043
Negative regulation of transferase activity	4	0.046

Supplemental Figure I

Supplemental Figure I: CXCL10 mRNA expression timecourse. mRNA expression in vascular spheroids was measured by quantitative RT-PCR after stimulation with trophoblast conditioned media (CM) for 8, 24 or 48 hours (n= at least 4). Data are expressed as mRNA expression relative to an external calibrator. All data are presented as mean + SEM. * Denotes $p < 0.05$ relative to control spheroids.

Supplemental Figure II



Supplemental Figure II: CXCR3 protein is expressed by first trimester decidua and co-localises with α -smooth muscle actin protein expression**A: CXCR3** and **B: α -smooth muscle actin** protein expression was examined by immunohistochemistry in serially sectioned first trimester decidua (n=5; representative image shown). CXCR3 and α -smooth muscle actin protein co-localised to the same cells (indicated by arrowheads). Negative control (inset) was incubated with non-immune IgG in place of primary antibody, scale bar represents 50 μ m. Both proteins were present at a time of trophoblast invasion as shown by positive **CK7** immunohistochemistry (**C**).